

# The Study of Biofunctionalization of Carbon Nanotubes and their Applications in Biology

Mustafa Aidin, Hedyeh Tafreshi, Husam Ali\*

Department of Chemistry, HiTech Institute of Theoretical and Computational Chemistry, India  
Department of Chemistry, Baghdad University of Technology, Baghdad, Iraq

Received: 13 March 2020

Accepted: 26 April 2020

Published: 01 June 2020

## Abstract

A carbon nanotube is a tube-shaped material, made of carbon, having a diameter measuring on the nanometer scale. A nanometer is one-billionth of a meter, or about one ten-thousandth of the thickness of a human hair. Carbon nanotubes have many structures differing in length, thickness, and in the type of helicity and number of layers. Although they are formed from essentially the same graphite sheet, their electrical characteristics differ depending on these variations, acting either as metals or as semiconductors.

Since their discovery in 1991, carbon nanotubes have generated huge activity in most areas of science and engineering due to their unprecedented physical and chemical properties. No previous material has displayed the combination of superlative mechanical, thermal and electronic properties attributed to them; these properties make nanotubes ideal, not only for a wide range of applications but as a test bed for fundamental science.

The tubular, vesicle-like character of carbon nanotubes has been used for drug containment and focused drug delivery in clinical trials (e.g., for the dispersal of cancer drugs for localized tumor treatment). Consequently, carbon nanotubes are also amenable for nano-sized platforms, whereby functional groups that would normally not coincide (e.g., like antibodies, polyethylene glycol, and cancer medication) can be brought together. Functionalization, through the attachment of different functional groups, has also made it possible to create nanotube-based moieties with complex behavior (e.g., a drug-delivery vehicle that can traverse the plasma membrane, and release the drug in a target organelle).

**Keywords:** Carbon Nanotubes, Nanotoxicity, Silver Nanoparticles, Fullerene, Cytotoxicity, Surface Functionalization

## How to cite the article:

M. Aidin, H. Tafreshi, H. Ali, *The Study of Biofunctionalization of Carbon Nanotubes and their Applications in Biology*, Medbiotech J. 2020; 4(2): 70-82, DOI: 10.22034/MBT.2020.109582.

©2020 The Authors. This is an open access article under the CC BY license

## 1. Introduction

Nanomaterials have emerged as potential tools in almost every field from space to the environment and from health to robotics. With the increasing demand for nanomaterials it is necessary to evaluate toxicity carefully before accepting new nanomaterial in wider bioapplications. In this chapter, technical developments on carbon

nanotubes are described with an account of their historical development, experimental models and potential applications. The first section describes the carbon nanotubes-based nanocomposites. This chapter is divided in subsections on the toxic nature of CNT, model CNT-metal and collagen composites, structure of carbon nanotube materials, physical principles of CNT-biosurface interaction, nanoindentation testing and the mechanism of

\* Corresponding Author E-mail: husam.ali@gmail.com

inflammation in epithelial cells induced by CNT with an account of biophysical experiments on CNT exposed to mesenchymal cells, 3D human lung prototype, skin tissues and prototype scaffold nanomaterials. A possibility of CNT as a safer drug delivery system is explored that describes the future of possible bioapplications of carbon nanotubes and nanocomposites [1-3].

Carbon nanotubes were discovered in 1991 and their use expanded to make conductive and high-strength composites, energy storage devices, sensors and actuators, field emission displays, nano-scale semiconductor devices, probes with unique physical, mechanical, electrical, and thermal properties. Initially CNTs in powder form were considered to be cytotoxic and DNA mutagenic with risk of inhalation-induced toxicity to workers due to direct skin contact. Several studies recently indicated possible toxicity of CNTs based on the facts that: 1) CNTs and fullerenes have produced toxic effects on biological systems ; 2) CNTs can translocate to bloodstream ; 3) CNTs can cross blood brain barrier ; and 4) toxicity of CNTs results in pulmonary inflammation as the main effect on tissues due to the distinct shape and biodegradation properties of CNTs [4-6].

Donaldson *et al.* described in detail three main properties of CNTs associated with pathogenicity of particles. The properties were:

- 1) CNTs showed more toxicity than larger sized particles,
- 2) fiber-shaped CNTs behave like asbestos and other pathogenic fibers which have toxicity associated with their needle-like shape, and
- 3) biologically biopersistent particles. Authors also pointed out that CNTs are possibly one of the least biodegradable man-made materials ever devised. Other concerns over the increased emissions of CNTs into the environmental compartments (air, water and soil) were due to improper disposal of CNTs. With all these concerns, now safe use of carbon nanotube material is emerging as state of the art since it was found biocompatible with hard bony material and nanoscale source of drug delivery carrier in the body. Present view of CNTs is perceived as nanomaterial with double face because of CNT induced toxicity and possibility of safer biomedical applications of new CNT nanocomposites. However, science is still discovering new methods of CNT nanocomposite preparations and toxicity testing of carbon nanotubes and CNT composites in biomedical applications [7-9].

### 1.1 Carbon Nanotubes (CNTs) and Other Carbon Nanomaterials Applications

Carbon nanotubes (CNTs) and other carbon nanomaterials are of interest for biological and medical applications because of their high chemical

durability, mechanical strength and electrical properties. Several studies on the application of carbon nanomaterials have been reported such as CNT substrates of cell culture, CNT-based drug delivery systems, and medical CNT implant materials. A recent study reported the synergy on the unique properties of carbon nanotubes (CNT) with details of tissue compatibility and osteogenesis of human mesenchymal stem cells (hMSC). It is believed that CNTs will provide an exciting opportunity for novel therapeutic modalities. However, little is known about the impact of CNTs on cellular processes such as adhesion, proliferation, and differentiation of mesenchymal cells (MSC). The following questions emerged on the interaction between CNT based nanomaterial and MSC cells [10-12] :

1. How are CNT-based composites are prepared and tested for physical properties on surface of CNT-based nanocomposites?
2. How do CNT-based composites affect cellular processes (e.g., renewal, metabolic activity, and differentiation) of MSCs?
3. Which stages of cell division during differentiation of stem cells are most affected by CNT-based materials?
4. Does addition of CNTs into naturally derived polymers result in creating stiffer environment in which progenitor MSC cells may prefer to differentiate into matured cells such as osteocytes, myocytes, hepatocytes?

Changes in cellular and physiological properties of MSC including adhesion, proliferation, and differentiation are major tests of toxicity during cellular processes. CNT-based nano substrates are black in color with low optical transparency for optical microscopic observation of the cultured MSC cells fixed on the CNT-based substrates. Collagen-SWCNT composites are better alternatives. Single-walled CNTs (SWCNTs) substrates in cell culture are strongly entrapped by collagen in composite. Collagen based composites showed high mechanical strength and good cell viability. Type I collagen is one of the most biocompatible materials. Collagen-coated cell culture dish is widely used for cell culture. CNTs show a high affinity for the collagen-coated dish surface [13-15].

MSC cells serve as incorporated experimental cells in scaffold preparation. Scaffold serves as a living-tissue analog consisting of cells embedded in a collagen-CNT matrix. The application of collagen-CNT matrix is now growing in biological applications. An intriguing point was that augmenting the properties of naturally derived collagen polymers through incorporation of CNTs might enhance *in vitro* osteogenic and osteoblastic

differentiation of MSCs. In the following the sections, we will describe *in situ* microscopic observation of cultured MSC cells in interaction with CNTs to evaluate the CNT-induced toxicity.

### 1.2. Physical Principles of Carbon Nanotube Surface Science

Physical principles of carbon nanotube surface science were explored in detail over a decade. Carbon nanotube surface property was considered peculiar in enhancing the surface area exposed to any tissue or biological exposure. Physical properties were considered as markers of CNT toxicity characteristics such as electrical conductivity of single-walled or multiwalled CNT material.

Consider the Drude model in which the electrical conductivity is given by  $\sigma = eN\mu$  where  $e$  is the absolute value of the electron charge,  $N$  is the spatial carrier density, and  $\mu = e\tau/m^*$  denotes carrier drift mobility which, in turn, reads  $\mu$  where  $\tau$  designates relaxation time (or momentum-scattering rate) and  $m^*$  stands for carrier effective mass. Then, by replacing the second formula with the first one, it follows [16, 17]:

$$\sigma = e^2 N \tau / m^* \quad (1)$$

Equation (1) is standard in the physics of semiconductors and constitutes a relevant element of reference within the context of macroscopic condensed-matter systems. In particular, let us consider a multiwalled carbon nanotube (MWCNT) conceived as a longitudinal quantum box according to Mooney *et al.* and Durkop *et al.* in such a tube, conductance is quantized according to the fact that the involved quantum number coincides with the numbering of the CNT layers (conductance scales with the number of layers). Therefore, quantizing formula (1) for a metallic MWCNT, conductivity due to the  $n^{\text{th}}$  layer will be [18]:

$$\sigma_n = e^2 N_n \tau_n / m \quad (2)$$

Where  $n$  designates quantum number ( $n = 1, 2, \dots$ ) and  $m^*$  has been replaced by the free-electron mass denoted by  $m$ . In addition, now  $\tau_n$  is transit time or motion time (if MWCNT transport is ballistic) so  $E_n = \hbar^2 n^2 / (8 ml^2)$  that  $\tau_n = l / v_n$  where  $l$  is the length of the tube and  $v_n$  stands for the magnitude of the quantized Fermi velocity which, for  $n \gg 1$ , approaches the electron velocity deduced from equating the quantized electron energy (corresponding to the electron confinement in the carbon nanotube as a longitudinal ideal quantum box) to  $(1/2) m v_n^2$ . Hence, it follows:

$$v_n = \hbar n / 2ml \quad (3)$$

Where  $\hbar$  is the Planck constant.

We regard our MWCNT as a quasi-one-dimensional structure so that  $A^{1/2} \ll 1$  where  $A$  is the cross-sectional area of the tube. On the other hand, we assume that the number of electrons participating in the conduction process depends upon  $n$  in accordance with the distribution of electrons in the atomic shells so that the above number equals  $2n^2$ . Therefore, inserting the relation, namely  $N_n = 2n^2 / (lA)$  in Equation 2, taking in account that the quantized conductance is given by  $G_n = \sigma_n A / l$ , and inserting it into equation relations 2 and 3 with the fact that  $\tau_n = l / v_n$ , final output is:  $G_n = 2G_0 n$  where  $G_0 = 2e^2 / h$  is the fundamental conductance quantum. The abovementioned expression for the quantized conductance of MWCNT indicates that conductance approximately depends linearly on  $n$  which is acceptable in the quasi-classical case, that is, for sufficiently large values of the quantum number. At any rate, a formula valid for every  $n$  can be given. To get this, we use the following relationship concerning the energy-level spacing induced by quantum confinement, namely [1, 19, 20]:

$$E_{n+1} - E_n = \hbar v_{Fn} / 2l \quad (4)$$

where  $v_{Fn}$  is the magnitude of the quantized Fermi velocity. By Equation 4 and the expression for the quantized energy, one gets:

$$v_{Fn} = \hbar(2n+1) / 4ml \quad (5)$$

Notice that the right-hand side of Equation 3 coincides approximately with the right-hand side of Equation 5 when  $n \gg 1$  (quasiclassical case). Repeating the calculation process in light of the Drude model developed previously by employing new Equation 5 for the electron velocity, the quantized conductance can be expressed as [1, 21, 22]:

$$G_n = 4kG_0 n^2 / 2n+1 \quad (6)$$

Where  $k$  is a phenomenological parameter such that  $k < 1$  which is a measure of the interwall (interlayer) coupling in the CNT tube. We assume that  $A$ : is a uniform continuous random variable so its average or expected value is  $\langle k \rangle = 1/2$ . In the quasi-classical case, that is, when  $n \gg 1$ , from relationship it follows that  $G_n \sim 2kG_0 n$  which gives an expected observed value. The above explanation and results of multiwalled nanotube surface agree

with the experimental data as demonstrated by Grado-Caffaro *et al.* 2008 [10, 13, 15].

### 1.3. Motivation - Combining Nanotechnology and Surface Science with Growing Bioapplications

**Carbon nanotubes:** In recent past fullerenes, nanotubes showed potential applications due to their large surface area and free radical chemistry, their strong attraction to electrons, and antioxidant properties. The combination of nanotechnology and surface science toward heterogeneous catalysis was a promising challenge for both technical applications and fundamental research, which is still in its infancy, even more than nanoelectronics. Successful combination of these complementary research areas has resolved some mysteries such as some Carbon-60 fullerenes bind to nucleotides, and hamper self-repair in double-strand DNA.

In addition, these CNT materials have high electrical and thermal conductivity, high strength, and rigidity. Medical/nonmedical applications further suggested the occupational, accidental exposure with enormous economic impact. Fullerenes (CNT cages), single-wall nanotubes, and multiwalled CNT nanotubes may show cytotoxicity. On the other hand, these materials were reported as nontoxic and protective against pathologies of acute or chronic neurodegeneration and liver diseases. Major concerns emerged because CNT produced superoxide anion, lipid peroxidation, and cytotoxicity in plants and animals. Uncoated fullerenes in largemouth bass showed lipid peroxidation in brain tissue and glutathione depletion in gills.

It makes a difference if CNT nanomaterial is metal or oxide as shown in inhalation studies. CNT material has promising applications as a component of chemical catalysts for chemical processes such as alcohol oxidation in direct liquid fuel cells, hydrogen-related technology, or Fischer-Tropsch synthesis, and CNT may provide sustainable energy sources for the future. Using CNTs as strong support material is a promising approach. Multiwalled CNT materials are used as models for porous materials and a rare two-dimensional biosystem for theoretical and applied studies. In this direction, remarkable progress is made. In the following section, preparation and physical characterization of metal-supported CNT-Ni, CNT-Si, CNT-Co composites and polymer supported CNT composites are described with an aim to achieve high value CNTs [1, 23, 24].

**Nanofabrication of CNT materials:** Metal-supported multiwalled CNT catalysts can be prepared by metal vapor deposition or by "wet-chemistry" procedures. The first technique leads to ultraclean materials pertinent for mechanistic studies. In the second approach, ultra clean material can be up-

scaled to synthesize bulk quantities. Bulk quantities of CNT-metal composite provide a larger dispersion of the nanometal clusters as realistic model systems for technical applications.

### 1.4. Cytotoxicity Measurement and Mechanisms of CNT Toxicity

In the last decade, several biophysical properties were investigated such as surface chemistry of membrane damage, protein denaturation, DNA damage, immune reactivity, macrophage action, inflammatory action of cells, and the reactive oxygen species showing specific changes in cells associated with size, mass, and surface area of carbon nanotubes. Molecular mechanisms of cytotoxicity caused by CNT are still not resolved and remain unconfirmed. The following section is a guideline to explain mechanisms of cytotoxicity of CNT composites. Nanotoxicity is caused after nanoparticles enter GIT by eating and drinking via mucociliary escalator in the respiratory tract. Mostly CNTs are excreted out by the bowel. CNT tube size and charge surfactant effect on CNT determine the CNT uptake and transport through liver, spleen, blood and brush border membrane. Upon ingestion of radiolabeled CNT by an animal, approximately 90% radiolabeled fullerenes remain in the body, 70% in the liver and the other 20% is excreted from the body. CNT functionalized with DTPA and radiotracer was quickly excreted from blood in mice (Half life = 3 and half hours). In a previous study, the aggregation property of CNT was reported important in toxicity and nano powder of Zn caused high mortality in mice, but micro powder of Zn did not show mortality. Based on previous reports, surface chemistry of CNTs plays a significant role in bioapplications as summarized in following section [25-27].

- Reactive oxygen makes reactive oxygen species of CNT, which causes toxicity to cells.
- Physical parameters such as size, mass, and surface area of carbon nanotubes play a determinant role and show specific effect on macrophage action, and inflammatory action of cells.
- Membrane damage, protein denaturation, DNA damage, immune reactivity are some leading examples of toxicity caused by surface coating of Zn, Cd, and Si around CNTs.
- Surface charge of polycations on membrane plays a significant role in toxicity. Charge density on the surface of CNTs nanostructures is associated with magnitude of toxicity.

Toxicity and structural details of fullerenes further suggest the problems and feasibility of accepting CNT and composites for bioapplications. Multiwall

CNT such as C60 showed toxicity due to surface modified by PVP to make highly stable charge transfer complexes. A similar concern was expressed that some fullerenes if suspended in solution by dissolving C60 in THF solvent may not pass through the blood brain barrier, while only THF may pass. Metal catalyst used in nanotube fabrication may be toxic, and sample preparation may exacerbate the toxicity of these metals. However, more derivatized fullerene structures are less toxic due to their low efficiency in ROS generation. Most of the single-walled and multiwalled CNTs are not water-soluble. CNT toxicity effects may range over seven orders of magnitude for different functionalizing CNT molecules. Aggregation in CNT derivatization on outer surface is important as interior surfaces of CNTs may be less derivatized or not at all derivatized. Sidewall CNT functionalization and low concentrations of CNT are always better options to reduce toxicity than using surfactant coating over CNT. Dose dependent epitheloid granuloma was reported for CNT material with formation of aggregates of nanotubes inside macrophages.

#### 1.4.1. *In Vivo Studies on CNT Toxicity*

With the advent of continuous monitoring of biological signals by real-time robust automated recording devices, it has become possible to measure CNT toxicity at nanoscale. Few reports are available about airborne CNT nanoparticles (NP) and dermal exposure of CNT and other nanometals. For interested readers, confirmed reports of other representative nanoparticles are illustrated in airway exposure and nanotoxicity to understand the toxicity mechanisms.

It is a known fact that inhalation of TiO<sub>2</sub>, carbon black, diesel toxicity causes inflammation, oxidative stress, and blood clotting ability. Approximately, 2.5-micron nanomaterial particles can reach in alveoli and may cause macrophage phagocytosis, and inflammation and nanoparticles may interfere with its clearance efficiency from alveoli. Translocation of nanoparticles is also greatly affected in the liver under influence of nonparenchymal cells. Conceptually, NP can go to the heart and can cause arrhythmia and coagulation. NP may also translocate through the olfactory nerve ending to the brain. Nanoparticles that usually cause inflammation and affect the autoimmune system are most likely to damage or alter tissues in the body such as skin, brain, liver, heart, blood, lymph node. Recent studies showed TiO<sub>2</sub>, ZnO nanoparticle ROS generated and microbeads can get to the dermis and lymph nodes where proteins affect the autoimmune system. Submicron-sized NP can get through via hair follicles. Small NP may interact with the immune system [18, 28].

Conceptually, nanoparticles in semiconductors create an electronhole pair and are detected by photon absorption in UVA or UVB regions. Such behavior indicates that the electron-hole pair acts with water and makes ROS, singlet oxygen, and superoxide. In following the section, we will describe an account of the inflammation testing protocol of alveolar epithelial cells and mechanism of CNT toxicity in lung fibroblasts initially reported by Stoker *et al.*

#### 1.4.2. *Inflammatory Mechanism of CNT Cytotoxicity*

Inflammatory mechanism of CNT cytotoxicity was explored in detail by several investigators in pulmonary inflammation. Monolayer cultures of epithelial, fibroblasts and smooth muscle cells were ideally used as experimental control of the system to test toxicity of CNTs without any cell-cell interactions. Dexamethasone and VEGF controlled delivery was visualized across the fibroblast-embedded collagen gel as multimodal dynamic model to simulate human airways. The inflammatory lung reactions (alveolitis) were used as the source of genetic lesions, which could eventually lead to the development of lung cancer. Another *in vitro* model of the airway was reported with culturing epithelial cells as monolayer on a membrane and fibroblasts as a monolayer at a fixed distance away separated by culture media. *In vivo* studies were performed using guinea pigs and rats. In a recent study, investigators showed the appearance of multifocal granulomas, resulting in inflammatory reactions of the terminal and respiratory bronchials with mild fibrosis in the alveolar septa.

Another study reported an improved model of fibroblasts following unique characteristics: 1) It maintains the normal anatomical arrangement (orientation and dimensions) of epithelial and fibroblast cells; 2) The fibroblast was embedded in collagen I, yet remained anchored; 3) A thin (10  $\mu$ m) porous polyester membrane separated the epithelial and fibroblast cell layers to allow communication between the epithelium and fibroblast to investigate cell specific protein expression following exposure to external perturbation. Kwon *et al.* (2009) further established the role of Nitric oxide (NO) produced by many cells in the body. Under normal (basal) conditions, NO was continually produced by cNOS (constitutive nitric oxide synthase). However, during inflammation, the amount of NO produced by iNOS can be a 1000-fold greater than that produced by cNOS in basal condition. Investigators predicted that NO production measurement could identify the level of inflammation in co-culture system [18, 20].

However, the pitfalls of fullerene structures are that they have high binding and high activation

energies with a high possibility of binding CNT with circulating free molecules such as hormones, enzymes, peptides and ions. Microimaging showed clearly that the epidermis layer of the skin was a prime target of CNT, and CNT can affect the viable skin cells while they are used as drug carriers. Our other direction of CNT effect on live alveolar cells was to observe the inflammatory changes in cultured fibroblast cells. The synergy of cytokines, nitric oxide production and cytotoxicity of alveolar cells were the main alterations caused during CNT exposure to alveolar cells. The transepithelial electrical resistance of alveolar cells was a unique index identified as CNT induced cytotoxicity biomarker without changing the drug delivery properties.

The fullerenes are main CNT constituents. They are bound with drugs at their hydrophilic  $-C-COO^-$  or  $-NH^+$  or SH sites. The pH, temperature, concentration and charge of drug molecules in blood are the main factors of controlled rate of drug delivery.

Mesenchymal stem cells (MSC) serve as model culture to study cytotoxicity. In a previous study, MSC were isolated from rats femurs under aseptic conditions and the excised connective tissue or epiphyses were removed from the femurs and the cavity was washed twice with phosphate buffered saline (PBS) solution with 1% penicillin/streptomycin to remove bone marrow.

#### 1.4.3. Characterization and Toxicity of SWCNT and MWCNT Carbon Nanotubes

The high-purity single-walled carbon nanotubes (SWCNTs) serve as nanomaterial available from Carbon Nanotechnologies Inc, prepared by HiPCO process with residual metal content 3-12% by weight, individual nanotubes 0.8-1.2 nm in diameter and 100-1000 nm in length. To prepare nanomaterial, SWCNTs are added to distilled water, and the mixture may be sonicated for 60 minutes using Sonicor 3000 manufactured by Misonix (Farmingdale, NY). Other study reported formation of nanoropes from nonionic octylphenol ethoxylate surfactant, Triton™ X-100 added to the dilute aqueous SWCNT solution to facilitate the separation of individual nanotubes.

The degree of SWCNT dispersion in the aqueous solution is ideally evaluated using an atomic force microscope (AFM) MultiMode II developed by Veeco Digital Instruments Group (Woodbury, NY). MTT assay (colorimetric assay for assessing cell metabolic activity) was used to evaluate the changes in cellular metabolic (mitochondrial) activity of cells as a cytotoxic response. Cells were exposed to varying concentrations of SWCNTs after 48 hours. In brief, 150  $\mu$ L of MTT (5 mg/ml) was added to each well and incubated for 4 hours. Afterward, 850  $\mu$ L of the MTT solubilization solution (10% Triton X-100 in 0.1 N HCL in anhydrous isopropanol) was

added to each well. The resulting formazan crystals was solubilized in acidic isopropanol and quantified by measuring absorbance at 570 nm. Data were calibrated to the appropriate calibration curve as stated in Sigma protocols as described by Kwon *et al*, 2009. Formation of formazan crystals represents the toxicity of CNT.

Measurement of Transepithelial Electrical Resistance (TER) is a new development used in isolated cells. Investigators reported human bronchial epithelial cells grown at the interface of air and liquid. In this technique, culture media was provided from the bottom through the porous membrane. TER of human bronchial epithelial cell with fibroblasts-embedded collagen layers cultured in Transwell™ was monitored using a portable Voltohmmeter (Millipore, Bedford, MA) attached to a dual "chopstick" or transcellular resistance measurement chamber (Millipore, Bedford, MA). In brief, different concentrations of CNTs were exposed to the co culture layers for 6 hours. Each of the two electrode systems contained Ag/AgCl electrode for measuring voltage and a concentric spiral of silver wire for passing current across the epithelium. Electric current passed across the epithelium was used to measure TER ( $\text{ohms}\cdot\text{cm}^2$ ). TER values higher than the background fluid resistance indicated a confluent airway epithelium with enlarged cell-cell tight junctions due to CNT toxicity. TER was monitored to identify the perturbation in the normal physiology and permeability due to CNT toxicity on human bronchial epithelial cells [13, 14, 29].

Metabolizing enzymes or intracellular enzymes such as alkaline phosphatase, leucine aminopeptidases, hepatic lysosomal enzymes, esterases are other targets involved in CNT induced cellular changes. Enhanced enzymes represent the cell differentiation, phagocytosis and proliferation in cells and measurement methods of intracellular enzymes.

Hypoxia state of cells is another form of cytotoxicity testing to capitalize the potential of hypoxia in measuring the cytotoxicity effect of CNT on epithelial cell survival. Initially, hypoxia induced by CNT was estimated by clonogenic assay of clonogenic cell survival. Oxygen pressure measurement of poor oxygenation in tumor cells is other method of cytotoxicity testing. Hypoxia was measured in tumor cells using OxyLite pO<sub>2</sub> system (Oxford Optronix Ltd, UK) attached with four oxygen probes implanted in mice tumors to measure tumor oxygen by using fluorescence quenching technique under neuroleptanalgesia of animals placed in thermal blanket at 37°C. For 10 minutes, probes measured the 100 PO<sub>2</sub> readings in tumor cells. Radiopharmaceutical radiolabeled nanoparticles are now mostly evaluated by

measuring oxygen pressure of cells at different locations in tumors.

#### 1.4.4. Cell proliferation measurement

Cell proliferation assays provide information of fast cell divisions induced by CNTs in contact. The rate of cell proliferation may be measured using the Picogreen dsDNA bioassay kit (Invitrogen, CA). Cellular DNA concentration from cell lysate represents the nuclear integrity and its slow degeneration or programmed cell death indicates the apoptosis in cell. Cell proliferation and apoptosis assays distinguish the cell damage from necrosis if it occurs due to severe cell injury by CNTs on epithelial cells.

Multiwalled MWCNTs may make composite MWCNT-collagen materials. Baktur *et al.* (2010) established a technique of MWCNT collagen composite preparation at fixed concentration of collagen Type I (1 mg/ml) mixed with MWCNTs. Different MWCNTs forms included MWCNTs, MWCNTs-OH, MWCNTs-COOH, with two different sizes (OD: 20 - 30 nm. Length: 0.5 - 2.0 urn, 10 - 30 urn). Originally, MSCs were seeded on the different types of MWCNT collagen scaffolds and method was described. Investigators believe that MWCNTs-collagen scaffolds significantly enhanced the differentiation of MSCs at 10 ppm. In another study, investigators showed that all types of MWCNT-collagen scaffolds induced the higher level of MSC differentiation compared to controls.

#### 1.5. Surface functionalization of carbon nanotubes using metal nanoparticles

Surface functionalization of carbon nanotubes has been extensively carried out to modify their intrinsic properties and develop applications in various areas. Many functional species, such as biomolecules or metal nanoparticles (NPs) have attracted much attention since they enable us to make nanotubes for sensors, fuel cells, and templates for novel structure construction. Especially, Au NPs have been actively studied due to their interesting optical properties and strong affinity to biomolecules. A lot of methods for attaching Au NPs to carbon nanotubes have already been reported. JIANG *et al.* used cationic polyelectrolyte for negatively charged Au NPs to nitrogen-doped multi-walled carbon nanotubes (MWNTs). CARILLO *et al.* attached Au NPs noncovalently by coating nanotube surfaces with multilayered polymeric films. Similar results with electrostatic attachments using cation-modified or polymer-coated MWNTs have also been reported. From Raman scattering spectroscopy of the Au-functionalized suspended SWNTs, enhanced Raman scattering properties are obtained. The results suggest that the attached Au NPs may

contribute to the enhancement of resonant phenomena.

#### 1.5.1. Experimental Method for single -walled CNTs functionalized with Au NPs and Amino groups

SWNTs were grown using a cold-wall CVD chamber. Ar and methane were the carrier gas and carbon feedstock, respectively. Plane and patterned SiO<sub>2</sub> (100 nm)/Si substrates were used for SWNT growth. All substrates were rinsed thoroughly with a piranha solution, a mixture of H<sub>2</sub>SO<sub>4</sub> and H<sub>2</sub>O<sub>2</sub> (with volume ratio of 70%:30%), before ferritin spin casting. The ferritin solution (Sigma-Aldrich) was diluted using deionized water (18.2 MΩ) and the final concentration was adjusted to 0.05 and 5 mg/mL. To obtain catalytic nanoparticles, ferritin solution was dropped onto the substrates using a spinner with a rotation condition of 600 r/min for 30 s and 4 000 r/min for 3 min. After then, substrates were rinsed with deionized water and calcined at 450 °C for 5 min in air.

Typical growth was carried out at 900 °C for 5 min at  $6.7 \times 10^4$  Pa under the constant flow of 300 mL/min. the SWNTs formed network structures on patterned substrates [23, 27, 28, 30] .

To chemically oxidize the sidewall of the suspended SWNTs, as-grown samples were immersed in a mixture of H<sub>2</sub>SO<sub>4</sub>+H<sub>2</sub>O<sub>2</sub> for 3 min. After rinsing with deionized water, the suspended SWNTs were immersed in the mixture of EDC and NHS solution for 5 min. This process produces NHS esters on the SWNTs surface. To covalently couple with amine groups, the SWNTs were immersed in ethylenediamine solvent for 10 min. Then, the suspended SWNTs were briefly rinsed with toluene and dried at 100 °C for 10 min in air. Finally, 30 μL of aqueous Au colloid was dropped on the suspended SWNTs. After incubation for 2 h, samples were dried by nitrogen-gas blow.

Optical properties of Au-attached suspended SWNTs since Au NPs are known as excellent Raman enhancers and SWNTs also show a strongly surface-enhanced Raman scattering (SERS) phenomena when they are in contact with specific metals. The high intensity ratio of the disorder-related D-band (around 1 300 cm<sup>-1</sup>) to the G-band (around 1 590 cm<sup>-1</sup>) means that as-grown SWNTs have high quality Figure 1.

In lower frequency region of Raman spectra, observed enhanced peak frequency and strong peak intensity in the non-resonant region after Au functionalization. Raman spectra from the pristine and Au functionalized SWNTs showed a clear difference in the line shape before and after Au attachment. The pristine samples produced sharp G-band and Breit-Wigner-Fano (BWF) shoulder, which are characteristics of semiconducting and metallic tubes, respectively.

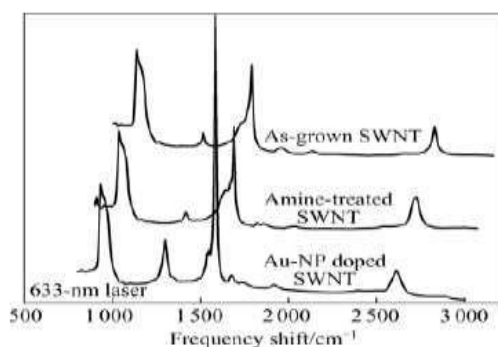


**Figure 1.** Representative Raman Profiles showing drastic among as-grown, amine treated and Au - functionalized suspended SWNTs in high frequency region (Excitation wavelength of 633 nm).

In contrast, suppression of the semiconducting component (around  $1590\text{ cm}^{-1}$ ) and a significantly enhanced G-peak intensity (around  $1590\text{ cm}^{-1}$ ) were observed after Au functionalization's-FET devices using a standard device fabrication process and investigated their electronic transport properties [15, 30].

#### 1.6. An efficient route towards the covalent functionalization carbon nanotubes

One-dimensional growth of materials to form nanowires and nanotubes has attracted tremendous interest in recent years. Among various classes of high aspect ratio nanostructures of inorganic and organic materials, carbon nanotubes (CNTs), especially single walled carbon nanotubes (SWNTs) have proven themselves as an extremely promising class of nanostructured materials for diverse applications like molecular electronics, chemical sensing, gas storage, field-emission, scanning microscopy and catalysis. However, their lack of solubility and difficulty in processing as thin films in solvents have imposed many barriers for their widespread use in many of these applications [4, 19, 27, 30].

One way to overcome these barriers is by using chemical functionalization to alleviate these processing difficulties or alternatively to explore the possibility of using CNT-polymer composites where hopefully, some of the attractive features of polymer processing can be brought in. Unfortunately, many studies of polymer-CNT nanocomposites, however, reveal segregation and non-uniform mixing behavior often causing serious concerns of reproducibility in their electrical, mechanical and thermal behavior. Many composites show different types of threshold behavior in terms of change in electrical, thermal or mechanical properties with the amount of CNT and the properties of composites critically depend on the miscibility, mixing, compatibility and adhesion. For example, recently a remarkable in situ

preparation of nylon-CNT composites has been reported to show that tailoring of the CNT polymer interfacial interaction could alter the morphology and properties. However, in all these cases chemical functionalization is an essential prerequisite to get uniform properties of the composites. Thus, in order to take the full advantage of the remarkable geometrical structure of CNT in various applications, especially using in the form of many robust polymer composites, CNTs need to be solubilized or derivatized with inorganic or organic functional groups that facilitate a strong bonding and selectivity through either hydrogen or covalent bonds. Many approaches have been tried so far to carry out chemical functionalization of carbon nanotubes. For example, the generation of surface hydrophilic substituents such as carboxylic, hydroxyl or sulphonic acid groups by suitable chemical method is rather easy for their wide use in medical and biological applications; since, these functional groups provide necessary sites for covalent or non-covalent coupling of SWNTs. In addition to the improvement of the performance of SWNTs, the development of new functionalization methods is of immense importance, since through proper functionalization it is possible to impart improved or altogether new, unique properties like non-toxicity or biocompatibility, which could be essential for biological applications. Consequently, a majority of recent reports deal with a variety of chemical treatments such as fluorination, alkylation, diazotization, use of organic radicals or nitrenes for sidewall functionalization although many methods still need greater efforts in order to improve the yield and selectivity of the products.

A simple and efficient method of chemical functionalization of both single and multiwalled carbon nanotubes has been discussed to give enhanced water solubility by rapidly and efficiently generating an appreciable amount of hydrophilic functional groups using microwave radiation. Surface functionalization containing more than 30 wt% of oxygen has been achieved, resulting into solubility of 2–5 mg/mL. Further covalent functionalization of such soluble SWNTs provides a remarkable degree of aniline functionalization through amidation, where the formation of polyaniline has been avoided. Further functionalization of these soluble SWNTs using aniline is reported by a novel intermediate acylation strategy for a facile covalent amide linkage in presence of oxalyl chloride. Also, the direct mixing of a mineral acid shows evidence for the electrostatic interaction between aniline and s-SWNTs, where the acid plays a catalytic role to form such interactions at ambient conditions [18, 19, 23, 31].

### 1.6.1. Experimental Method for covalent functionalization carbon nanotubes

#### Microwave assisted solubilization of SWNTs

The raw SWNTs (60% purity) used, were purchased from Aldrich with an average diameter of 0.8–1.4 nm and 5–100 mm length. MWNTs were synthesized by CVD using xylene–ferrocene mixture using 6 mol% of ferrocenes. Fifty milligrams of the as received SWNT/MWNT sample was taken in a 100 mL Teflon reaction chamber containing 50 mL of 1:1 mixture of oleum and 70% nitric acid. The Teflon lined reaction chamber was sealed with Teflon stopper made with grooves and made leak proof using a Teflon tape. Extreme care was taken during handling of such corrosive and strong oxidative mixture. The microwave power of about 420 W was used for the present studies with two cycles [1-min on then 1-min off]. The off time allowed the mixture to cool down. No external pressure was applied in this study, since a domestic microwave oven without pressure–temperature program, was used in the present case. A good dispersion of nanotubes with enhanced solubility has been achieved when the reaction time was fixed to 4 min. The contents were filtered through a 10 mm poly(tetrafluoroethylene) (PTFE) membrane and the black powder collected was again mixed 2 M HCl and ultrasonicated (33 kHz) for 20 min in order to convert  $-\text{COO}^-$  to the  $-\text{COOH}$  for further amine functionalization. The acid mixture containing dispersion of SWNTs/MWNTs was then filtered through 0.2 mm PTFE filter paper. On irradiation of microwave for 4 min to SWNTs gives optimal solubility with a minimal loss of nanotubes, MWNTs requires 5 min for their appreciable dispersion and solubility. The CNTs collected on filter paper were transferred to a dialysis bag with a cutoff molecular weight of 12 kDa. The bag was filled with 100 mL deionized water and subjected for the dialysis for 48 h. The deionized water used for the dialysis was frequently replaced in order to completely eliminate all acid residues from the CNT sample (till pH changes to 7). The suspension was removed from the bag and rota-vapped under vacuum to isolate into solid material for further characterization.

SWNTs and MWNTs functionalized by such microwave irradiation are symbolized as s-SWNTs and s-MWNTs, respectively, for the convenience of representation. Interestingly, the solubility of s-SWNTs was found to decrease with addition of an acid (four different mineral acids viz., HCl, H<sub>2</sub>SO<sub>4</sub>, HNO<sub>3</sub> and HClO<sub>4</sub> were used to check the effect. This effect of suppression in solubility of SWNTs in water could be due to the protonation of  $-\text{COO}^-$  moieties from the side-walls to form comparatively less soluble  $-\text{COOH}$  groups. On the other hand, the solubility was found to be little enhanced with

increase in pH, perhaps due to the formation of soluble salt of  $-\text{COO}^- \text{Na}^+ / \text{K}^+$  [10, 12, 32].

### 1. Surface amidation of s-SWNTs using aniline

About 20 mg of s-SWNTs having 2–3 mg/mL solubility was ultrasonicated for 10 min in presence of 10 mL of oxalyl chloride (taking extreme care during handling of oxalyl chloride) and the reaction was carried out in an argon atmosphere. The mixture was then refluxed for 24 h at 60 °C to obtain a higher degree of acylchloride functionalization (SWNTs-COCl); excess of oxalyl chloride was removed under vacuum using rota-evaporation. SWNTs-COCl was then mixed with 5 mL of pure and distilled aniline and refluxed at 190 °C (bp of aniline: 186 °C) for 40 h. The reaction was carried out in a closed and inert condition in order to avoid the oxidation of aniline. Excess of aniline was then removed by washing with copious amount of toluene with successive ultrasonication and centrifugation. The resultant SWNT-COHNHC<sub>6</sub>H<sub>5</sub> (15 mg) was characterized by FTIR, TGA and UV-vis spectroscopy; electrochemical studies were carried out using cyclic voltammetry and impedance spectroscopy.

### 2. Zwitterionic linkages between SWNTs and aniline

Upon the addition of amine to such s-SWNTs, the solubility of nanotubes gets suppressed due to the formation of linkages like SWNT-COO-H<sub>3</sub>N<sup>+</sup>R. This kind of bonding is rather different from usual amide linkages. In order to obtain such electrostatically amine functionalized SWNTs, 10 mg of s-SWNTs in 12 mL of deionized water was ultrasonicated for 10 min to form a clear black solution. To this solution, 1 mL of aniline hydrochloride was added and stirred gently and then ultrasonicated for 2 min. A black precipitate of SWNTCOO<sup>-</sup>H<sub>3</sub>N<sup>+</sup>C<sub>6</sub>H<sub>5</sub> settled down within few seconds, which was then washed thoroughly with deionized water and characterized by FTIR and TGA [24, 28, 33, 34].

### 1.7. Functionalization of multi-walled carbon nanotubes by epoxide ring-opening polymerization

Covalent functionalization of carbon nanotubes (CNTs) was accomplished by surface- initiated epoxide ring opening polymerization because of their insolubility and weak dispersibility in common solvents and matrices have limited their applications an effective method to prevent aggregation of nanotubes is functionalization of CNTs. The functionalization of CNTs by polymers may be divided into two categories on the basis of either noncovalent or covalent bonding between the CNTs and polymer. Further- more, covalent attachment of polymers will help to disperse CNTs.

Functionalization of single-walled and multi-walled CNTs by ring-opening polymerization was reported. Using this approach, polymer functionalized CNTs have been prepared using  $\epsilon$ -caprolactam,  $p$ -dioxanone, 3-ethyl-3-(hydroxymethyl)oxetane,  $\epsilon$ -caprolactone, and  $L$ -lactide as monomers. The structures of functionalized CNTs were characterized by Fourier transform infrared (FT-IR), thermogravimetric analysis (TGA), scanning electron microscopy (SEM), and transmission electron microscopic (TEM) techniques.

### 1.7.1. Experimental

Fifty milligrams of acid treated CNT (A-CNT), 400 mg of epichlorohydrin, and 50 mg of 40% NaOH aqueous solution were placed in a 50 mL round-bottomed flask equipped with a reflux condenser and the mixture was stirred for 3 h at 60, 70, and 80 °C, respectively. The mixture was filtered and the black solid was washed with acetone and deionized water several times. Finally, the product was dried in a vacuum oven at 100 °C for 24 h. The samples prepared are referred to as F60-CNT for reaction temperature of 60 °C, F70-CNT for reaction temperature of 70 °C, and F80-CNT for reaction temperature of 80 °C, respectively figure 2.

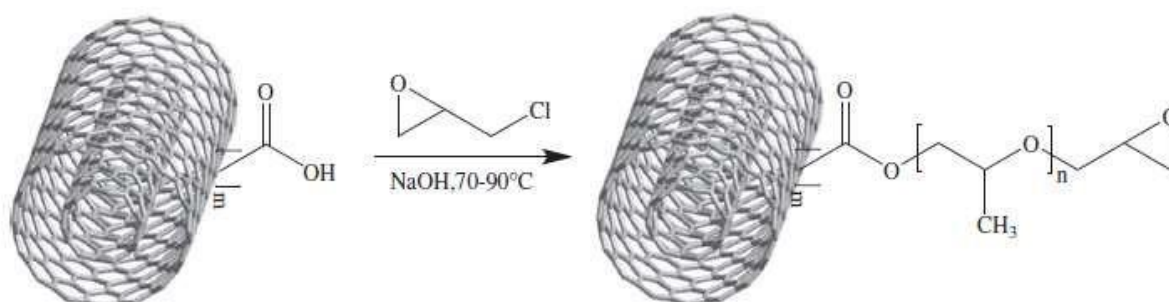


**Figure 2.** Procedure for functionalization of CNT by epoxide ring-opening polymerization [18].

For example Functionalization of multiwalled carbon nanotubes (MWNTs) with biodegradable supramolecular polypseudorotaxanes has been successfully performed by utilizing surface-initiated ring-opening polymerization of  $\epsilon$ -caprolactone (CL) to yield poly( $\epsilon$ -caprolactone)-grafted MWNTs (MWNT-g-PCL), followed by forming inclusion complexes between grafted-PCL chains and  $\alpha$ -cyclodextrins ( $\alpha$ -CDs) to give  $\alpha$ -CD-NTPCL hybrids. There are significant differences in the morphology and solubility of MWNTs before and after introduction of  $\alpha$ -CD. Some protuberances are clearly observed for  $\alpha$ -CD-NTPCL as compared with MWNT-g-PCL. Furthermore, the host-guest stoichiometry (monomeric unit of CL/ $\alpha$ -CD molar ratio) for  $\alpha$ -CD-NTPCL is much higher than that of polypseudorotaxanes consisted of linear PCL and  $\alpha$ -CDs. This observation can be explained by a combination of several reasons including the steric hindrance of grafted-PCL, the competitive exclusion between adjacent PCL chains toward  $\alpha$ -CD, and the addition order of  $\alpha$ -CD as well as the host-guest feed ratio. The present methodology may open up a new opportunity toward the application of supramolecular chemistry for the chemical manipulation and processing of CNTs. Moreover, such novel supramolecular hybrids provide an entry to extend the applications of CNTs to medicine and biology fields through embedding the functional polymers and heterogeneous components [27, 29, 35].

### 1.8. MSCs (Mesenchymal stem cells) Differentiation and Proliferation on Different Types of Scaffolds

MSC cells differentiate into osteocytes by slow process of osteogenesis on surface of MWCNT scaffolds in presence of collagen or plastic composite material in scaffolds. The progress of osteogenesis was sensitive to released alkaline phosphatase concentration from MSC cells in medium. Alkaline phosphatase enzyme concentration serves as biomarker of MSC differentiation and osteogenesis to compare the quality and biocompatibility of MW-CNTs in scaffold support material.

Another important cellular process is proliferation of MSCs represented by DNA concentration in MSCs exposed to different CNT Scaffolds. The MSC cell proliferation was related with type of MWCNT-collagen scaffold. Inflammatory and cytotoxic responses in MSCs were observed by increased nitric oxide (NO) production following exposure of increased concentration of single-walled carbon nanotubes (SWCNTs) to epithelial cells. At higher concentrations of SWCNTs, MSC cells showed cytotoxic response and portions of cell layers were detached as reported elsewhere. Each of the NO production rate was normalized by total proteins. Cellular metabolic activity was observed following exposure of different concentrations of SWCNTs to both MSC cell layers. MTT activity in MSC cells was decreased with increased concentration of SWCNTs, especially for epithelial cells.

### 1.8.1. Static Model: 3-Dimensional Tissue Engineered Lung

In laboratory, a prototype of monolayered epithelial cells cocultured with fibroblast-embedded collagen gel was designed to simulate human airway. Fibroblasts contract the extracellular matrix to close a wound and function perfectly upon placed in collagen gel. The model served as ideal example of isolated mediators participating in epithelial-fibroblast communication. It had several features: 1) It places the normal anatomical orientation of epithelial and fibroblast cells; 2) Fibroblasts embedded in anchored collagen I separated by 10 micrometers polyester membrane serves the purpose to study cell-specific protein expression or communication between epithelium and fibroblasts exposed to CNTs.

The co-culture technique in this review offers several distinct advantages over earlier models. The airway epithelial cells are cultured as a monolayer over a thin (10 mm) porous polyester membrane. A thin lung fibroblast embedded collagen layer was attached to the opposing side of membrane. In this fashion, the epithelial cells and fibroblast cells maintain the normal anatomical arrangement, but the polyester membrane allows easy separation of the cell types for cell-specific gene expression and proteomics analysis. Fibroblast-embedded Collagen I gels were prepared using rat-tail tendon collagen (RTTC; Collaborative, Bedford, MA, USA). Normal human lung fibroblasts (NHLF) were harvested upon reaching 75-80% confluence, and added (seeding density of  $5 \times 10^4$  fibroblasts/mL of final volume) to an iced mixture of collagen (final concentration 2.0 mg/ml), 5 concentrated DMEM, and 10X reconstitution buffer comprised of NaHCO<sub>3</sub>, HEPES buffer (Gibco, Grand Island, NY, USA) and NaOH. Aliquots of the mixture were pipetted onto the underside of a 1 cm<sup>2</sup> Transwell (Costar, Cambridge, MA, USA) polyester membrane (0.4 um pore). The outer rim of the membrane was fitted with a highly porous polyethylene ring. The liquid gel then swept into the porous ring at the edge and upon "gelling" was able to keep the fibroblast embedded gel from contracting. The collagen mixture was then allowed to "gel" (non-covalent crosslink) at 37°C in 5% CO<sub>2</sub> for 10-15 minutes. Harvested primary human bronchial epithelial (HBE) cells were then seeded ( $1.5 \times 10^5$  cells/cm<sup>2</sup>) directly on top of the polyester membrane. The entire tissue was submerged in media for 5 days and the epithelium was allowed to attach and become confluent. For the first 48 hours, the media was basal epithelial growth medium (BEGM, Clonetics, USA) and a low retinoic acid concentration. For days 3-5 (and days 6-21), the media was a 50:25:25 mixture of BEGM:DMEM:Hams F12 with a high retinoic acid

concentration. At day six, an air liquid interface was established (media maintains a high retinoic acid concentration) and the epithelium was allowed to differentiate for approximately two weeks at which time it is ready for experimentation [13, 16, 17, 25].

### 1.8.2. Dynamic Model: Integration of 3D Engineered Tissues into Cyclic Mechanical Strain Device

Dynamic cell growth condition served as more realistic *in vitro* viable alternative to *in vivo* model. We established a dynamic cell growth environment to mimic the dynamic changes in the amount of circumferential and longitudinal expansion and contraction that occur during normal breathing movement in the lung. Flex cell Tension Plus system can also be used to implement 5% cyclic equiaxial elongation, which is equivalent to 45% of total lung capacity, and the amount of stretching experienced during normal breathing condition. Patel and co-workers showed the differences in cellular responses (cell proliferation, cellular inflammation, reactive oxygen species (ROS), and glutathione (GSH)) to air pollutants including CNTs between dynamic and static cell growth environments, and demonstrated that implementing dynamic cell growth conditions was a closer approximation of *in vivo* conditions. This study provided one of the alternative ways to evaluate CNT-induced effects on human respiratory systems and a detailed insight for the development of a viable alternative to existing static *in vitro* or *in vivo* tests.

## References

1. Asemave K, Abakpa DO, Ligom TT. 1999. Extraction and Antibacterial Studies of Oil from three Mango Kernel obtained from Makurdi - Nigeria. *Progress in Chemical and Biochemical Research* 3(1): 74-80. en.
2. Sharma A, Khare S, Gupta M. 2002. Enzyme-Assisted Aqueous Extraction of Peanut Oil. *Journal of the American Oil Chemists' Society* 79: 215-218.
3. Huang J, Rozelle S, Pray C, Wang Q. 2002. Plant Biotechnology in China. *Science* 295(5555): 674.
4. Baccarani M, Martinelli G, Rosti G, Trabacchi E, Testoni N, Bassi S, et al. 2004. Imatinib and pegylated human recombinant interferon- $\alpha$ 2b in early chronic-phase chronic myeloid leukemia. *Blood* 104(13): 4245-4251.
5. Pulz O, Gross W. 2004. Valuable products from biotechnology of microalgae. *Applied Microbiology and Biotechnology* 65(6): 635-648.
6. Ahmadi M, Vahabzadeh F, Bonakdarpour B, Mofarrah E, Mehranian M. 2005. Application of the central composite design and response surface methodology to the advanced treatment of olive oil processing wastewater using Fenton's peroxidation. *Journal of Hazardous Materials* 123(1): 187-195.

7. Ibrahim HM, Yusoff WMW, Hamid AA, Illias RM, Hassan O, Omar O. 2005. Optimization of medium for the production of  $\beta$ -cyclodextrin glucanotransferase using Central Composite Design (CCD). *Process Biochemistry* 40(2): 753-758.
8. Gonçalves C, Carvalho JJ, Azenha MA, Alpendurada MF. 2006. Optimization of supercritical fluid extraction of pesticide residues in soil by means of central composite design and analysis by gas chromatography-tandem mass spectrometry. *Journal of Chromatography A* 1110(1): 6-14.
9. Davarnejad R, Kassim K, Ahmad Z, Sata S. 2008. Supercritical fluid extraction of  $\beta$ -carotene from crude palm oil using CO<sub>2</sub>. *Journal of Food Engineering - J FOOD ENG* 89: 472-478.
10. Ryan SM, Mantovani G, Wang X, Haddleton DM, Brayden DJ. 2008. Advances in PEGylation of important biotech molecules: delivery aspects. *Expert Opinion on Drug Delivery* 5(4): 371-383.
11. Sunarso J, Ismadji S. 2009. Decontamination of hazardous substances from solid matrices and liquids using supercritical fluids extraction: A review. *Journal of Hazardous Materials* 161(1): 1-20.
12. Jalali-Heravi M, Parastar H, Ebrahimi-Najafabadi H. 2009. Characterization of volatile components of Iranian saffron using factorial-based response surface modeling of ultrasonic extraction combined with gas chromatography-mass spectrometry analysis. *Journal of Chromatography A* 1216(33): 6088-6097.
13. Kumagai M, Sarma TK, Cabral H, Kaida S, Sekino M, Herlambang N, et al. 2010. Enhanced in vivo Magnetic Resonance Imaging of Tumors by PEGylated Iron-Oxide-Gold Core-Shell Nanoparticles with Prolonged Blood Circulation Properties. *Macromolecular Rapid Communications* 31(17): 1521-1528.
14. Ghasemi E, Raofie F, Najafi NM. 2011. Application of response surface methodology and central composite design for the optimisation of supercritical fluid extraction of essential oils from *Myrtus communis* L. leaves. *Food Chemistry* 126(3): 1449-1453.
15. Le Goff A, Gorgy K, Holzinger M, Haddad R, Zimmerman M, Cosnier S. 2011. Tris(bispyrene-bipyridine)iron(II): A Supramolecular Bridge for the Biofunctionalization of Carbon Nanotubes via  $\pi$ -Stacking and Pyrene/ $\beta$ -Cyclodextrin Host-Guest Interactions. *Chemistry - A European Journal* 17(37): 10216-10221.
16. Jafari MH, Kashisaz S, Manna M. 2019. Effects of Nanoparticles on the Durability and Mechanical Properties of Concrete. *Journal of Computational and Theoretical Nanoscience* 16(1): 275-283.
17. Esmailmotlagh M, Basiri Z, Kheirabadi MA, Oveisi K. 2019. The Effect of Information and Communication Technology on the Professional Development of Teachers. *Journal of Computational and Theoretical Nanoscience* 16(1): 312-318.
18. Raja V. 2019. Preparation and Characterization of Nanohybrid of MoO<sub>3</sub> through Different Methods. *Medbiotech Journal* 03(04): 135-138.
19. Aadesariya MK, Ram VR, Dave PN. 2019. Investigation of phytochemicals in methanolic leaves extracts of *Abutilon pannosum* and *Grewia tenax* by Q-TOF LC/MS. *Progress in Chemical and Biochemical Research* 2(1): 13-19. en.
20. Kheirabadi MA, Jafari MH, Alizadeh F, Basiri Z, Oveisi K. 2019. Comparison and Satisfaction of Injured Management System for Students Athlete in the Sport Federations. *Journal of Computational and Theoretical Nanoscience* 16(1): 284-288.
21. Ferreira GMD, Ferreira GMD, Almeida GWR, Soares NFF, Pires ACS, Silva LHM. 2019. Thermodynamics of multi-walled carbon nanotube biofunctionalization using nisin: The effect of peptide structure. *Colloids and Surfaces A: Physicochemical and Engineering Aspects* 578: 123611.
22. Eissazadeh S, Jafari MH, Kashisaz S, Manna M. 2019. Investigation into the Behavior of Square Concrete-Reinforced Columns Under Axial Loading, Retrofitted by Fiber-Reinforced Polymer and Steel Jacket. *Journal of Computational and Theoretical Nanoscience* 16(1): 295-307.
23. Soltantabar Shahabedini A, Alinezhad Chamazketi M, Yaghoubi Nezhad A, Mostafavi SM. 2020. Electrophoretic removal of sodium dodecyl sulphate from peptide solution through a hydrogel-micropipette system. *Eurasian Chemical Communications*. en.
24. Kashisaz S, Basiri Paknafs Z, Riahi A. 2020. The Milling of Metal through Adaptive Neuro-Fuzzy Inference System (ANFIS) for non-touch Measuring of the Temperature to Reduce Coolant. *Journal of Modern Processes in Manufacturing and Production* 9(2): 23-30.
25. Shamsin Beyranvand H, Mirzaei Ghaleh Ghobadi M, Sarlak H. 2020. Experimental Study of Carbon Dioxide Absorption in Diethyl Ethanolamine (DEEA) in the Presence of Titanium Dioxide (TiO<sub>2</sub>). *Progress in Chemical and Biochemical Research* 3(1): 55-63. en.
26. Ogbuagu AS-M, Okoye CI. 2020. Physico-chemical characterization of Avocado (*Persea americana* Mill.) Oil from Tree Indonesian Avocado Cultivars. *Progress in Chemical and Biochemical Research* 3(1): 39-45. en.
27. Basak G, Hazra C, Sen R. 2020. Biofunctionalized nanomaterials for in situ clean-up of hydrocarbon contamination: A quantum jump in global bioremediation research. *Journal of Environmental Management* 256: 109913.
28. Chai L, Tsamos MK, Tassou AS. 2020. Modelling and Evaluation of the Thermohydraulic

- Performance of Finned-Tube Supercritical Carbon Dioxide Gas Coolers. *Energies* 13(5).
29. Hwang J-Y, Shin US, Jang W-C, Hyun JK, Wall IB, Kim H-W. 2013. Biofunctionalized carbon nanotubes in neural regeneration: a mini-review. *Nanoscale* 5(2): 487-497.
30. Chemat F, Abert Vian M, Ravi HK, Khadhraoui B, Hilali S, Perino S, et al. 2019. Review of Alternative Solvents for Green Extraction of Food and Natural Products: Panorama, Principles, Applications and Prospects. *Molecules* 24(16): 3007. PubMed PMID: 31430982. eng.
31. Safoora Eissazadeh MHJ, Sara Kashisaz, Mohsen Manna. 2019. Investigation into the Behavior of Square Concrete-Reinforced Columns Under Axial Loading, Retrofitted by Fiber-Reinforced Polymer and Steel Jacket. *Journal of Computational and Theoretical Nanoscience* 16(01): 295-307.
32. Kheirabadi MA, Rahimi G, Zamani A, Alizadeh F, Basiri Z, Oveisi K. 2019. The comparison between the attitudes of employees and clients towards organizational intelligence (case study: Isfahan General Directorate of Sports and Youth). *Revista Latinoamericana de Hipertension* 14(1): 62-69.
33. Kheirabadi MA, Jafari MH, Alizadeh F, Basiri Z, Oveisi K. 2019. Making an entity-relationship model of the knowledge management process with strategic thinking. *Revista Latinoamericana de Hipertension* 14(1): 55-61.
34. Haddad R, Cosnier S, Maaref A, Holzinger M. 2009. Non-covalent biofunctionalization of single-walled carbon nanotubes via biotin attachment by  $\pi$ -stacking interactions and pyrrole polymerization. *Analyst* 134(12): 2412-2418.
35. Santharaman P, Venkatesh KA, Vairamani K, Benjamin AR, Sethy NK, Bhargava K, et al. 2017. ARM-microcontroller based portable nitrite electrochemical analyzer using cytochrome c reductase biofunctionalized onto screen printed carbon electrode. *Biosensors and Bioelectronics* 90: 410-417.